

Dimension-Adaptive Imaging with a SwarmSAR of Lightweight S-Band Nodes

Iannini, Lorenzo; Dogan, Ozan; Hoogeboom, Peter; Lopez Dekker, Paco

DOI

[10.1109/IGARSS47720.2021.9553428](https://doi.org/10.1109/IGARSS47720.2021.9553428)

Publication date

2021

Document Version

Final published version

Published in

2021 IEEE International Geoscience and Remote Sensing Symposium IGARSS

Citation (APA)

Iannini, L., Dogan, O., Hoogeboom, P., & Lopez Dekker, P. (2021). Dimension-Adaptive Imaging with a SwarmSAR of Lightweight S-Band Nodes. In *2021 IEEE International Geoscience and Remote Sensing Symposium IGARSS: Proceedings* (pp. 1098-1101). Article 9553428 IEEE.
<https://doi.org/10.1109/IGARSS47720.2021.9553428>

Important note

To cite this publication, please use the final published version (if applicable).
Please check the document version above.

Copyright

Other than for strictly personal use, it is not permitted to download, forward or distribute the text or part of it, without the consent of the author(s) and/or copyright holder(s), unless the work is under an open content license such as Creative Commons.

Takedown policy

Please contact us and provide details if you believe this document breaches copyrights.
We will remove access to the work immediately and investigate your claim.

Dimension-Adaptive Imaging with a SwarmSAR of Lightweight S-Band Nodes

Lorenzo Iannini, Ozan Dogan, Peter Hoogeboom, Paco Lopez-Dekker
Delft University of Technology, Delft, Netherlands

Abstract—Distributed SAR systems provide imaging capabilities that cannot be achieved by traditional monolithic satellites, thanks to the multiple angles and times of observation. In this paper the opportunities offered by a swarm of small satellite nodes operating in S-Band are discussed. The nodes fly in a close formation and operate in MIMO mode. All the N satellites transmit and receive the N pulses at the same time, following a Frequency Division Multiplexing (FDM) scheme. The work focuses in particular on the impact of the cross-track baselines on the resolution and on the quality of the signal reconstructed from the N^2 channels. A first iteration of a distributed target processor based on adaptive frequency and channel treatment is hence proposed with the aim of effectively accounting for the slope-induced spectral shifts.

I. INTRODUCTION

Multi-channel systems represent the future of Synthetic Aperture Radars (SAR) as they enable a more efficient use of the available antenna subsystems in terms of imaging products and performance. The next generation big satellites will for instance exploit digital beam forming to achieve high resolutions and wide swaths (see e.g. NISAR). It can be however argued that the most intriguing aspects of multi-channel systems are the advanced observation capabilities, such as target height and velocity estimation, that are offered by multi-platform systems. Among these latter, distributed SAR concepts based on a multiple-transmitters/multiple-receivers (MIMO) scheme are receiving a special interest as they provide a quadratic increase in the number of channels, and hence in the performance, with the number of nodes [1], and at the same time they enhance the system in terms of robustness to components faults and of cost-effectiveness. The redundancy and the power of single-platform systems can be in fact distributed among the nodes.

This paper debates the 3D imaging opportunities and the processing strategies associated to a swarm in N nodes flying in close formation, also recalled as SwarmSAR. The system operates in a MIMO configuration where the nodes are simple, i.e. they are equipped with a single transmit/receive module, and they have equal capabilities. All the N nodes transmit at the same time, with the same Pulse Repetition Frequency (PRF), and receive all the N transmitted pulses, generating a total of N^2 channels. The nodes would fly in a string-of-pearls formation, with a short along-track separation, that allows for coherent combination of the channels. The instruments illuminate the common footprint with a Frequency Division Multiplexing (FDM) strategy, as sketched in Fig. 1, ensuring the orthogonality condition between waveforms [2]. The N^2 boost factor in conventional 2D imaging is then given by a

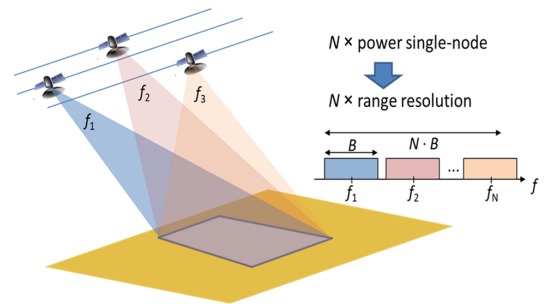


Fig. 1. Frequency Division Multiplexing scheme for the MIMO swarm constellation.

N increases in the range resolution as a consequence of the expanded bandwidth and by the augmented azimuth sample density (from the multiple receivers) that enhances the azimuth ambiguity performance and enables a larger aperture [3], [4], [5], as shown in Fig. 2. For cross-track and along track interferometry, the enhanced sensitivity is brought then by the N angle diversity.

In [6] the system philosophy and the overall imaging performance achieved by a single node and by the swarm were roughly outlined. The system was deemed suited to operate in S-Band (around 3 GHz frequency) for an overall convenience in terms of swath width, antenna simplicity and power requirements. It was found that 20 W of average radiated power are indeed sufficient to achieve a decent single-node performance. The present work will discuss in more detail the processing strategies for the high resolution imaging of distributed targets and the performance of the swarm for height estimation. The impact of the cross-track baselines and of the topography on such aspects is also explicitly addressed.

II. SWARMSAR CHANNELS

Different processing strategies can be envisioned depending on the product of interest. The N^2 channels can be focused separately and then combined or, alternatively, they can be merged at the raw data level. The first approach would be the most straightforward option for cross-track interferometry, whereas the latter shall be adopted for high resolution imaging. In either case the along-track (AT) and cross-track (XT) baselines between the satellites have to be properly accounted for. The XT baseline is in particular relevant in relation to the adopted FDM transmission scheme. Although the Tx waveforms are in fact orthogonal in the temporal frequency

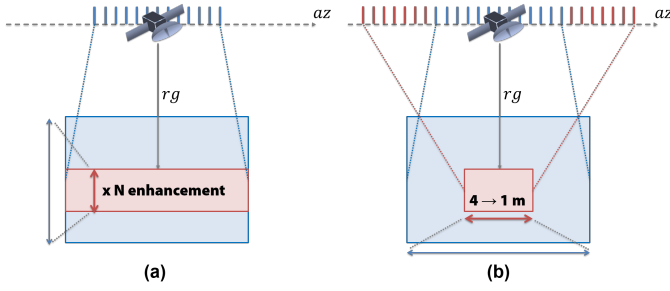


Fig. 2. Sketch representation of the resolution benefits from the swarm MIMO system. (a) The range resolution is improved by the increase in bandwidth from the FDM transmission scheme. (b) The increase in azimuth resolution is enabled by the possibility of increasing the integration aperture without degrading the azimuth ambiguity performance.

spectrum, some overlap is in general expected in the ground frequency spectrum, due to the well-known wavenumber shift [7]. The effect of the cross-track baseline, b , and of the local incidence angle, θ , on the shift Δf can be indeed quantified as

$$\Delta f_{ij,kl} = \frac{b_{ij,kl}}{R \tan(\theta)} f_0 \quad (1)$$

where R is the slant range, f_0 is the central frequency and where the local incidence angle shall be further expressed as $\theta = \theta_0 - \alpha$, i.e. as a function of the flat surface incidence θ_0 and of the local slope angle α . Notice that the perpendicular baseline between channels ij and kl , with i and k referring to the transmitter index and k and l to the receiver, shall be interpreted as the distance between the equivalent phase centers of the channels. It can be therefore expressed as

$$b_{ij,kl} = \frac{b_k + b_l}{2} - \frac{b_i + b_j}{2} \quad (2)$$

where the b_i are baselines with respect to any arbitrary orbit. For the S-band system parameters in Table IV, a shift of 1.25 MHz for 100 m baseline shall be therefore expected. This has a practical consequences on the channels processing as well as on the strategies to assign the frequencies to the N nodes. The two configurations illustrated in Fig. 3 for a $N = 2$ system convey that a variation in the total effective bandwidth, and hence the resolution, is expected from the sign of the baseline or, dually, by switching the satellite frequencies. The impact on the slant range resolution of the baselines intuitively is reduced for larger node bandwidths and for larger N , as it can be evinced from the 6-satellite example in Fig. 4. From (2) and from the figures, it can be also be inferred that the bistatic channels of adjacent bands have adjacent ground spectra support, which conveniently prevents the occurrence of large gaps. A marginal gap, with respect to the single node bandwidth, shall be instead put into account in order to prevent the overlap of the temporal spectra. When the monostatic channels converge, instead of diverging, an enhancement in the signal quality shall be expected within the frequency bands experiencing more channel overlap. In order to exploit this

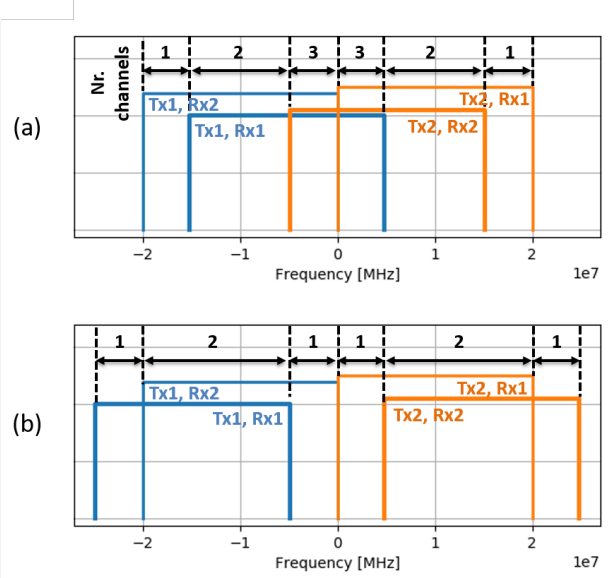


Fig. 3. Ground spectrum supports for the channels of a SwarmSAR with 2 nodes. The reference is an equivalent virtual orbit half way between the two platforms. A 500 m cross-track baseline between the two platforms has been simulated with (a) height(node2) > height(node1) and (b) height(node2) < height(node1). The band portions used for the imaging processor and the associated number of channels are highlighted in black color.

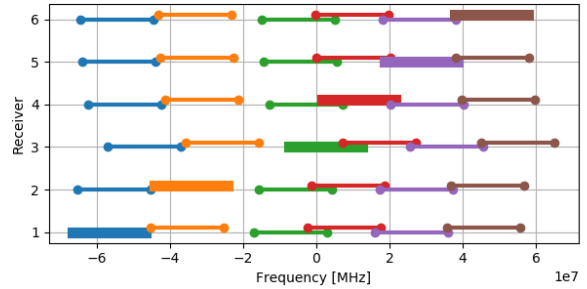


Fig. 4. Ground spectra for the channels of a SwarmSAR with 6 nodes and a baseline spread of 1 km. The baselines have been randomly assigned within such cross-track range. Different colors correspond to different transmitters. The thicker segments indicate the monostatic channels.

information, a frequency and channel adaptive approach is outlined for high resolution (HR) imaging and topography height estimation in the following two sections.

III. MIMO HR IMAGING

The signal reconstruction from multiple monostatic and bistatic channels is a well covered problem in the SAR literature (see e.g. [3], [5], [4], [8]). The coherent fusion of the N^2 swarm channels for HR imaging shall be performed at the raw data level. The channels have approximately the same doppler support. The approach herewith proposed assumes perfect knowledge on the orbits, and therefore on the baselines, and applies to both point targets and distributed targets. In light of the considerations in the previous section, it shall be in fact remarked that the complexity introduced is beneficial

for distributed targets, as point targets do not suffer from geometric decorrelation. The devised strategy accounts for the following steps:

- *Delineation of reference orbit.* The data are focused in the radar coordinates (slant range and azimuth) of a virtual orbit.
- *Delineation of spatial blocks.* The scene extent is divided in blocks that approximately share the same ground slope, basing therefore on a Digital Elevation Model (DEM).

For each block:

- *Delineation of coherent bands.* The overall ground frequency domain is segmented into B bands, with the criterion that each band should be fully covered by $N_{ch} > 0$ channels and that N_b should be minimized for the seek of efficiency. An example of such bands is provided in Fig. 3 for $N = 2$ scenario (with $N_b = 6$ bands delineated). A less computationally demanding procedure shall account for a minimum width of the bands, for $N > 2$. For each band the following steps shall be performed on the N_{ch} channels.

- *Range compression.* The compression facilitates the next step and enhances the robustness to thermal noise [9]

- *Removal of differential topography phase.* The spectral shift is applied to the channels by removing the phase difference with respect to the reference orbit (a mapping between the different slant ranges is also needed) along the whole azimuth history. Notice that in order to avoid Nyquist, the cross-track location of the reference orbit is generated at half-way between the two most distant satellites.

- *Band filtering.* The band portion of interest is isolated (band-pass filtered).

- *Antenna pattern calibration.* Before merging the channels the amplitude and phase differences caused by the gains and pattern variations between the antennas and to the along track baselines (for bistatic channels) has to be compensated.

For each pixel in the focused grid of the block:

- *Phase history compensation.* The azimuth signal of the range migrated cell is first extracted from the filtered channels through interpolation. The phase history model is then subtracted from the phase of such signal.

- *Channel reconstruction.* If $N_{ch} > 1$ the azimuth signals from the different channels are merged into a regularly sampled signal. This is done through the Best Linear Unbiased interpolator proposed in [10] and already exploited for the swarm in [11]. The different along-track baselines shall be properly accounted for.

- *Azimuth integration.* The samples are simply integrated along the aperture, since the phase history was removed in the previous step. This approach is in fact equivalent to a traditional back-projection.

The focused output from the N_b bands are then fused by simple summation to generate the high resolution image. The individual band outputs and the merged impulse response function of a target are shown in Fig. 5 for the scenario (a) of Fig. 3. With such processing, it can be intuitively predicted that the power of the azimuth ambiguities is frequency dependent, and it is expected to be higher in the bands covered by a single channel (that remain undersampled).

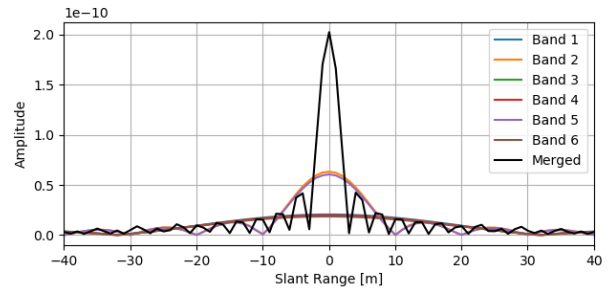


Fig. 5. Impulse response function of a point target from the $N = 2$ SwarmSAR with node specifications in Table IV. The output of the single bands delineated in Fig. 3 (sorted in ascending ground frequency order) is shown together with the band fusion (black line).

TABLE I
SWARM NODE SPECIFICATIONS

Parameter	Value
Frequency	3.2 GHz
Average Tr power	20W
Pulse Length	20 μ s
Antenna	Reflector \varnothing 2 m
Beam width	3.2 $^\circ$
Bandwidth	20 MHz
Orbit height	514 km
NESZ	- 19 dB
DTAR	- 18 dB

IV. MIMO INSAR

With MIMO InSAR we refer to single-pass InSAR for surface height estimation. The most straightforward (not necessarily optimal) choice to produce topography height products is to combine the channel after having them focused individually. A first iteration on the potential performance was provided by [6]. However, the problem was implicitly treated as a combination of SIMO systems, thus discarding the information carried by channels with different transmitters. Even if the common bandwidth between such channels is narrow and the height information achievable is at low resolution, such contributions should not be discarded. Figure 6 shows for instance that for large baselines channel pairs with different transmitters (with adjacent frequencies) have non-null coherence. We further analyze then the performance for the system in Table IV, characterized by NESZ and DTAR below -17 dB. The NRCS of the distributed target has been set to -15 dB. The standard deviation of the estimated height, shown in Fig. 7, conveys that the impact of the number of nodes is very significant especially for short baselines. With 6 satellites a relatively narrow baseline of 300 meters is sufficient to achieve 1 m accuracy on 20 m cell resolution, whereas 1.5 km baseline is required for 6 m resolution. It can be further observed that the performance still increases for very long baselines. This is indeed consistent with the intuitive fact that the N times larger bandwidth of the swarm leads to a N times larger critical baseline with respect to a single-transmitter scenario.

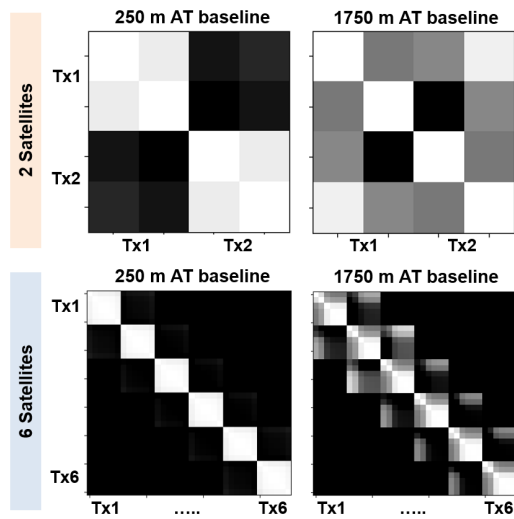


Fig. 6. Coherences between the N^2 channels, with $N = 2$ (top panels) and $N = 6$ (bottom panels), for two XT baseline configurations. In the first configuration (left panels) the two farthest satellites are 250 m distant, in the second (right panels) 1750 m. White and black colormap entries correspond to coherence values of 1 and 0 respectively.

V. DISCUSSION AND CONCLUSIONS

The paper elaborates on the effective strategies for FDM MIMO SAR imaging and analyses the performance for height information retrieval. Although the high resolution imaging and the InSAR products are discussed separately and the processing procedures follow two different routes, as the first is carried out on raw data and the latter on focused data, a common denominator can be nevertheless found. That is indeed provided by the attempt to exploit all the available coherent information for distributed targets, although the within-scene variations (dependent on the ground slope) of the spectral shift might make it more cumbersome. This effort represents indeed the main message of the paper. In addition, it shall be observed that the quality of the reconstruction methods for HR imaging is dependent on the DEM accuracy and that this latter would benefit from a higher azimuth ambiguity performance, achievable by exploiting multiple channels. The performance trade-off between these two information and the optimal strategy to achieve it (either through an recursive estimate procedure or a joint estimation) shall be further investigated.

VI. ACKNOWLEDGMENTS

The work presented in this paper was carried out at Delft University of Technology within the frame of the project *Dutch network on small spaceborne radar instruments and applications (NL-RIA)* funded by the Netherlands Organization for Scientific Research.

REFERENCES

- [1] G. Krieger, "Mimo-sar: Opportunities and pitfalls," *IEEE Transactions on Geoscience and Remote Sensing*, vol. 52, no. 5, pp. 2628–2645, 2014.

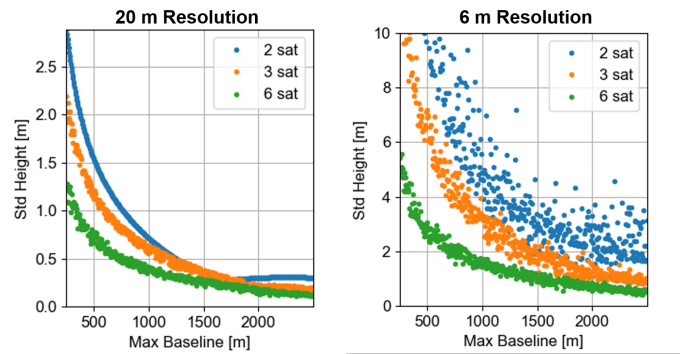


Fig. 7. Accuracy of surface height estimated by MIMO InSAR on ground resolutions of 6 and 20 meters as a function of the number of the XT baseline spread and the number of nodes.

- [2] G. Krieger, M. Younis, S. Huber, F. Bordonni, A. Patyuchenko, J. Kim, P. Laskowski, M. Villano, T. Romme, P. Lopez-Dekker, and A. Moreira, "Mimo-sar and the orthogonality confusion," in *2012 IEEE International Geoscience and Remote Sensing Symposium*, 2012, pp. 1533–1536.
- [3] G. Krieger, N. Gebert, and A. Moreira, "Unambiguous sar signal reconstruction from nonuniform displaced phase center sampling," *IEEE Geoscience and Remote Sensing Letters*, vol. 1, no. 4, pp. 260–264, 2004.
- [4] D. Cerutti-Maori, I. Sikaneta, J. Klare, and C. H. Gierull, "Mimo sar processing for multichannel high-resolution wide-swath radars," *IEEE Transactions on Geoscience and Remote Sensing*, vol. 52, no. 8, pp. 5034–5055, 2014.
- [5] Pietro Guccione, Andrea Monti Guarnieri, Fabio Rocca, Davide Giudici, and Nico Gebert, "Along-track multistatic synthetic aperture radar formations of minisatellites," *Remote Sensing*, vol. 12, no. 1, 2020.
- [6] L. Iannini, P. Lopez-Dekker, and P. Hoogeboom, "A highly flexible and scalable s-band swarmsar from very simple nodes," in *2020 IEEE Radar Conference (RadarConf20)*, 2020, pp. 1–6.
- [7] F. Gatelli, A. Monti Guarnieri, F. Parizzi, P. Pasquali, C. Prati, and F. Rocca, "The wavenumber shift in sar interferometry," *IEEE Transactions on Geoscience and Remote Sensing*, vol. 32, no. 4, pp. 855–865, 1994.
- [8] N. Sakar, M. Rodriguez-Cassola, P. Prats-Iraola, and A. Moreira, "Azimuth reconstruction algorithm for multistatic sar formations with large along-track baselines," *IEEE Transactions on Geoscience and Remote Sensing*, vol. 58, no. 3, pp. 1931–1940, 2020.
- [9] Muriel Pinheiro, Pau Prats-Iraola, Marc Rodriguez-Cassola, and Michelangelo Villano, "Analysis of low-oversampled staggered sar data," *IEEE Journal of Selected Topics in Applied Earth Observations and Remote Sensing*, vol. 13, pp. 241–255, 2020.
- [10] M. Villano, G. Krieger, and A. Moreira, "Staggered sar: High-resolution wide-swath imaging by continuous pri variation," *IEEE Transactions on Geoscience and Remote Sensing*, vol. 52, no. 7, pp. 4462–4479, 2014.
- [11] L. Iannini, A. Mancinelli, P. Lopez-Dekker, P. Hoogeboom, Y. Li, F. Uysal, and A. Yarovoy, "Prf sampling strategies for swarmsar systems," in *IGARSS 2019 - 2019 IEEE International Geoscience and Remote Sensing Symposium*, 2019, pp. 8621–8624.